Glass Formation in the Na₂O–TiO₂–P₂O₅ System

S. KRIMI,* A. EL JAZOULI,† L. RABARDEL,‡ M. COUZI,§
I. MANSOURI,* AND G. LE FLEM‡

*Département de Chimie, Faculté des Sciences Ain Chock, Casablanca,
Morocco; †Département de Chimie, Faculté des Sciences Ben M'Sik,
Casablanca, Morocco; ‡Laboratoire de Chimie du Solide du CNRS, UPR
8661, 351 cours de la Libération, 33405 Talence, France; and §Laboratoire
de Spectroscopie Moléculaire et Cristalline, URA 124 CNRS, 351 cours de
la Libération, 33405 Talence, France

Conditions of glass formation in the Na₂O–TiO₂–P₂O₅ system are reported. The largest quantity of TiO₂ which can be introduced is 35 mole%. Study of the recrystallization process leads to the identification of a new Nasicon-type phosphate, Na₅Ti(PO₄)₃. In glasses the Ti⁴⁺ ions are presumably located in both pyramidal and octahedral oxygenated sites. © 1993 Academic Press, Inc.

Introduction

Transparent glasses with relatively large nonlinearities are promising materials for all-optical switching applications. The choice of composition is mainly dictated by the possibility of an increase of the nonlinear index coefficient n_2 but one must consider also various parameters such as high damage threshold, ultrafast response time, and the wave guide fabrication process (1).

Little information is available for predicting nonlinear refractive index changes in glasses; thus a systematic investigation of the relation between glass composition and optical nonlinearities is of interest. An obvious guide for selecting glass components is to choose entities with high hyperpolarizabilities for the network and highly polarizable cations as modifiers.

From a recent analysis of the nonlinear refractive index in crystals by Adair et al.

(2), the most significant result is the high value of n_2 found for titanium oxides containing TiO₆ octahedral entities. In a recent publication Vogel et al. studied the optical nonlinearities in a series of four-component TiO₂, Nb₂O₅, Na₂O, and SiO₂ systems and came to the conclusion that the nonlinear index coefficient is larger for Ti than for Nb doping (3).

Within this scope the present paper reports a preliminary investigation of glass formation in the Na₂O–TiO₂–P₂O₅ system. P₂O₅ was selected as the glass-forming oxide and sodium ions were introduced to make a possible ion exchange easier. The glass-forming region has been determined. Systematic investigation of the crystallization has allowed us to discover a new crystalline Nasicon-type related phase, Na₅Ti(PO₄)₃. Raman spectroscopy and EXAFS experiments were used to elucidate the structural

A $57.14Na_2O$-$42.86P_2O_5$
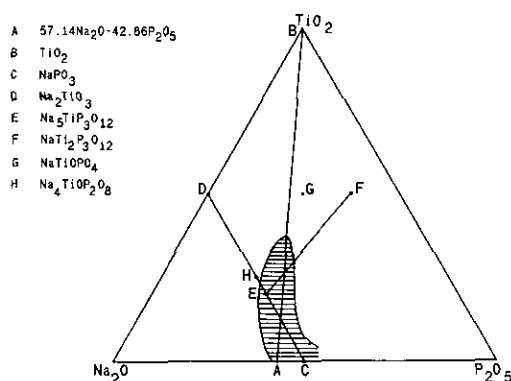B TiO_2
C $NaPO_3$
D Na_2TiO_3
E $Na_5TiP_3O_{12}$
F $NaTi_2P_3O_{12}$
G $NaTiOPO_4$
H $Na_4TiOP_2O_8$

FIG. 1. Domain of the nonhygroscopic glasses in the Na_2O–TiO_2–P_2O_5 system.

FIG. 2. Variation of the densities vs composition for the glasses of the AB line.

Experimental

Elaboration

The investigated glasses have molar compositions xNa_2O–$yTiO_2$–zP_2O_5. They were prepared from sodium carbonate dried at 400°C, titanium dioxide dried at 600°C, and diammonium hydrogen phosphate according to the reaction scheme $xNa_2CO_3 + yTiO_2 + 2z(NH_4)_2HPO_4 \rightarrow [xNa_2O, yTiO_2, zP_2O_5] + 4zNH_3 + 3zH_2O + xCO_2.$

The corresponding mixture introduced in a platinum crucible is heated for 24 hr at 200°C, allowing decomposition of the diammonium phosphate. The temperature was then progressively raised to 1100°C and held constant at this value for 20 min. The molten glasses were quenched in air and later annealed close to the glass transition temperature. Under these conditions all the glasses are colorless. The glass-forming region for nonhygroscopic samples (i.e., with low P_2O_5 content) is given in Fig. 1. It is almost identical with that previously reported (4).

Glass Forming Tendency

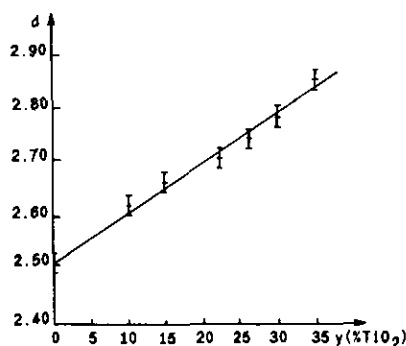The vitreous domain can be readily described by the line AB joining the points

corresponding to the composition Na_2O/P_2O_5 = 1.33 (A) and TiO_2 (B) and the line CD joining the points C ($NaPO_3$) and D (Na_2TiO_3) (Fig. 1). The largest quantity of TiO_2 introduced in the glass is 35 mole% between A and B and 22.5 mole% between C and D. These results are comparable with those previously reported in the systems Li_2O–TiO_2–P_2O_5. MgO–TiO_2–P_2O_5, and CaO–TiO_2–P_2O_5 (5). TiO_2 is easly incorporated into glasses containing 50 mole% P_2O_5 or less. The densities of the glasses increase with increasing proportion of TiO_2. Figure 2 gives the variation of densities vs TiO_2
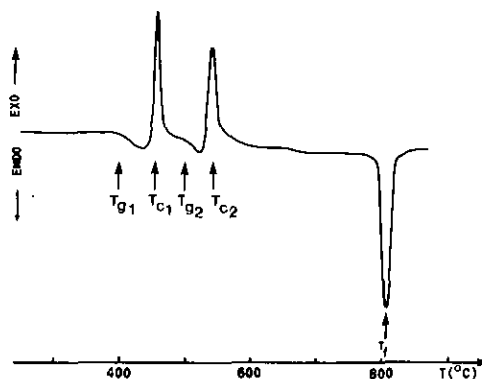
FIG. 3. DTA curve for the glass with composition 50 mole% Na_2O, 20 mole% TiO_2, 30 mole% P_2O_5.

TABLE I

PRODUCTS OF RECRYSTALLIZATION OF THE INVESTIGATED GLASSES

Glass compositions (mole%)			
Na_2O	TiO_2	P_2O_5	XRD detected phases above T_c
37.1	35	27.9	$NaTi_2(PO_4)_3$, $Na_4TiO(PO_4)_2$, $NaTiOPO_4$
40	30	30	$NaTi_2(PO_4)_3$, $Na_5Ti(PO_4)_3$, $Na_4P_2O_7$, TiO_2
44.5	22.2	33.3	$NaTi_2(PO_4)_3$, $Na_5Ti(PO_4)_3$, $Na_4P_2O_7$
50	22.5	27.5	$NaTi_2(PO_4)_3$, $Na_5Ti(PO_4)_3$, $Na_4P_2O_7$, TiO_2
50	20	30	$Na_5Ti(PO_4)_3$
50	15	35	"u," $Na_5Ti(PO_4)_3$, $Na_4P_2O_7$, $NaTi_2(PO_4)_3$
48.6	15	36.4	"u," $Na_4P_2O_7$
50	10	40	"u," $Na_4P_2O_7$
50	5	45	"u," $NaPO_3$

content for glass compositions along the AB line.

Recrystallization Process

The thermal properties were analyzed using differential thermal analysis (DTA) and calorimetric analysis. The processes of phase transformation for all samples are complex. As an example, Fig. 3 gives the DTA curve obtained for the glass with the composition 50 mole% Na_2O, 20 mole% TiO_2, and 30 mole% P_2O_5: two glass transitions are observed, respectively, at 414 and 507°C and two exothermic peaks at 454 and 525°C. The melting point is 787°C. For the heat treated glass at 454°C an admixture of $Na_4TiO(PO_4)_2$ and $Na_4P_2O_7$ in addition to a remaining vitreous phase were identified by XRD. Above 550°C only a new phase $Na_5Ti(PO_4)_3$, is detected. Actually a careful calorimetric analysis carried out between 500 and 550°C shows clearly two peaks located at 528 and 542°C: the first may correspond to the crystallization of the last vitreous phase while the second one can be associated wtih the formation of $Na_5Ti(PO_4)_3$.

In Table I are listed the products of recrystallization of all the investigated samples detected by XRD above the final temperature of recrystallization. All the phases but one (labeled "u") have been identified.

The Crystalline New Phosphate $Na_5Ti(PO_4)_3$

The crystalline form of $Na_5Ti(PO_4)_3$ can also be prepared by calcination of a mixture of Na_2CO_3, TiO_2, and $(NH_4)_2HPO_4$ in stoichiometric proportion. The pure compound is obtained after two thermal treatments of 15 hr at 300 and 500°C, respectively, and a final thermal treatment of 24 hr at 750°C. At room temperature the XRD pattern can be indexed assuming a hexagonal cell: $a = 9.0608(1)$ Å, $c = 21.734(1)$ Å ($Z = 6$, $d_{exp.} = 2.84$, $d_x = 2.89$). Actually, absent reflections $-h + k + l \neq 3n$ indicate a rhombohedral symmetry. Moreover, the observed reflections $h\bar{h}l$: $l \neq 2n$ are consistent with the $R32$ space group.

These data can be analyzed in the context of the Nasicon-type phosphates and related compounds. This structure was described for the first time by Hagman et al. for the $NaA_2(PO_4)_3$ (A = Ti, Ge, Zr) phosphates (6). It consists of a three-dimensional network formed by PO_4 tetrahedra sharing corners with AO_6 octahedra. The site occupied by the sodium atoms, usually labeled M_1, is an elongated octahedron sharing common triangular faces with two neighboring (AO_6) octahedra along the c-axis of the hexagonal cell. Within this structure three other sites (M_2) also exist that are normally available
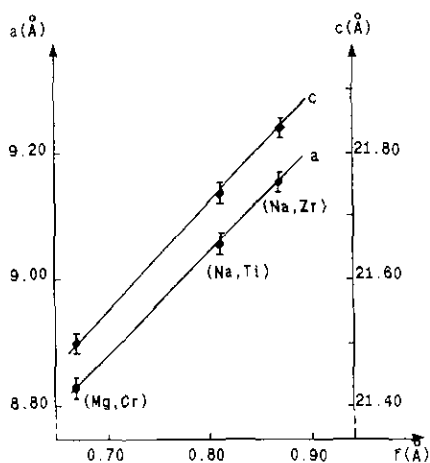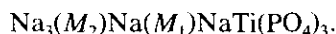
FIG. 4. Variation of the cell parameters and of the sodium rich Nasicon-type phosphates vs mean A^{n+} ionic radii [$Na_4MgCr(PO_4)_3$ (17), $Na_5Zr(PO_4)_3$ (18)].

for alkali cations. Schematically the usual crystal chemical formula can be written as $M_1(M_2)_3A_2(PO_4)_3$. The rules governing the cell parameter variations already have been established (7): (i) the c parameter increases with the size of the A^{n+} ion and the Na^+ $(M_1)-A^{n+}$ electrostatic repulsion; (ii) the a parameter is a function of the A^{n+} size and of the amount of Na^+ ions in the M_2 positions. Accordingly the following distribution for $Na_5Ti(PO_4)_3$ can be proposed:

$$Na_3(M_2)Na(M_1)NaTi(PO_4)_3.$$

The parameters of the cell are compared in Fig. 4 with those of sodium-rich Nasicon phosphates. A linear variation as a function of the A^{n+} mean size is observed. This is in agreement with the proposed cationic distribution.

Spectroscopic Investigation

Absorption Spectra

To illustrate the influence of titanium content on the optical transparency of these glasses, the absorption spectra were recorded for samples with compositions on

the AB line and also for the glassy and crystalline forms of $Na_5Ti(PO_4)_3$. The absorption threshold values are compared in Table II with those of the crystalline phases TiO_2, $SrTiO_3$, and $NaTi_2(PO_4)_3$.

The strong absorption results from the formal electronic transfer

$$O^{2-}(2p^6) + Ti^{4+}(3d^0)$$
$$\rightarrow O^-(2p^5) + Ti^{3+}(3d^1t_{2g}).$$
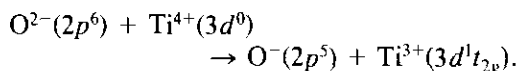
Its energy decreases as the amount of titanium increases in the glass and tends progressively toward that of TiO_2. Moreover, the value measured for the glassy form of $Na_5Ti(PO_4)_3$ is slightly below that of the crystal.

In $SrTiO_3$ the Ti–O bonds are more covalent than in TiO_2 due to the better overlap between $3d$ titanium and $2p$ oxygen orbitals and the reinforcement of the Ti–O bond by the antagonistic Sr–O ionic band.

In the Nasicon-type phosphates the ionic character of the sodium–oxygen bond is counterbalanced by the rigid phosphotitanium framework involving the strong Ti–O bond and accordingly high E values.

TABLE II

ABSORPTION THRESHOLDS (E) OF SEVERAL GLASSES OF THE $Na_2O-TiO_2-P_2O_5$ SYSTEM AND OF TYPICAL CRYSTALLINE PHASES

Glass compositions (mol%)			
Na_2O	TiO_2	P_2O_5	E(eV)
51.4	10	38.6	3.47
48.6	15	36.4	3.41
50	20	30 ($Na_5Ti(PO_4)_3$)	3.40
44.5	22.20	33.30	3.36
40	30	30	3.33
37.1	35	27.9	3.27

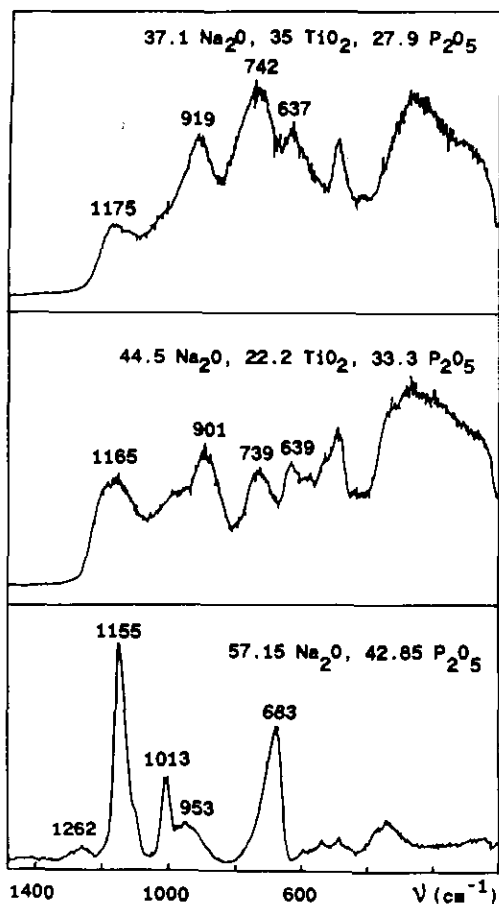| Crystalline phases			
TiO_2 (rutile) (9)			3
$SrTiO_3$ (9)			3.4
$NaTi_2(PO_4)_3$ (10)			3.54
$Na_5Ti(PO_4)_3$			3.50

FIG. 5. Raman spectra of glasses of the AB line.

The framework of the investigated glasses is made of PO_4 tetrahedral groups and TiO_n ($4 \le n \le 6$) entities and coexists with the sodium modifier ions. There is a clear relation between the increasing sodium content and the rising of E values which corresponds to the progressive strengthening of the Ti–O bonds. Thus the titanium oxygen entities in the poorest titanium glasses must contain the smallest Ti–O distances.

Raman Spectroscopy

The Raman spectra have been recorded on a Dilor Z 24 triple monochromator instrument. The 514.5-nm emission line of a Spectra Physics Model 171 argon ion laser was used for excitation with incident power of around 200 mW. Detection was made with a Hamamatsu cooled photomultiplier coupled with a photon counting system. The spectral resolution was about 2 to 3 cm^{-1}. The colorless glassy samples have been cut in the shape of parallelepipeds of about $5 \times 5 \times 5$ mm^3 with surfaces carefully polished.

The Raman spectra of the investigated glasses corresponding to the AB line are shown in Fig. 5. Examples of spectra exhibited by glasses of the CD and EF lines are given in Fig. 6. In addition, the spectra of $Na_5Ti(PO_4)_3$ in the crystalline and glassy forms are compared in Fig. 7. Tentative band assignment can be made on the basis of the previous data characterizing the sodium phosphates and the titanium oxygen bonds in crystals and glasses.

For the glasses free of TiO_2 the observed spectra are in fair agreement with those previously reported by Fawcett et al. (11). For instance, in sample A (Fig. 5) the bands are characteristic of metaphosphate chains with finite lengths. The weak line observed at
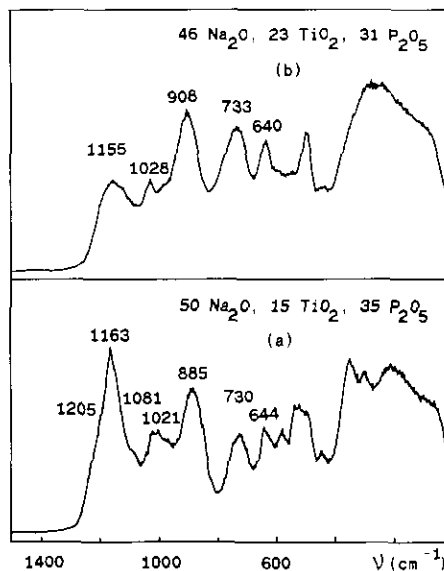

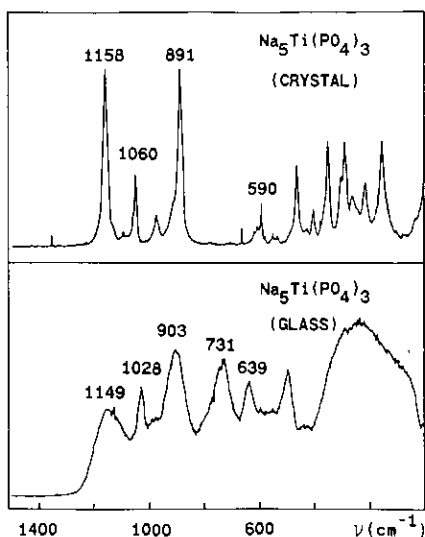FIG. 6. Raman spectra of glasses of the CD (a) and EF (b) lines.

FIG. 7. Comparison of the Raman spectra of both forms of $Na_5Ti(PO_4)_3$.

about 1260 cm^{-1} corresponds to the asymmetric PO_2 stretching mode and the strong one at 1155 cm^{-1} is due to the symmetric PO_2 stretch. The line at 1013 cm^{-1} is assigned to the symmetric stretching mode of PO_3 end groups of the metaphosphate chains. The broad band around 950 cm^{-1} and the strong one at 683 cm^{-1} are attributed to the asymmetric and symmetric P–O–P stretch, respectively.

As a general trend for one glass with its composition located along the AB (Fig. 5), CD, and EF (Fig. 6) lines, the introduction of TiO_2 leads to the appearance of broad bands peaking at about 900, 740, and 640 cm^{-1}. All these bands are observed for the glassy form of $Na_5Ti(PO_4)_3$. For all the samples containing the richest proportion of titanium, the high energy region becomes a broadband more or less resolved with a continuous decreasing of the peak intensity of about 1165 cm^{-1} ($\nu_S PO_2$).

Discussion

The Raman spectra of the $Na_2O-P_2O_5$ glasses are almost similar to the spectra of

the corresponding crystalline sodium phosphate: the symmetric PO_2 stretch frequency shifts to lower values as the sodium proportion increases. In pure sodium phosphate this evolution is associated with a reduction of the metaphosphate chain length. The same evolution is also observed in glasses containing larger proportions of TiO_2. Both the enlargement of the highest energy band and the decreasing intensity of the band peaking at about 1165 cm^{-1} are consistent with this interpretation.

The relation between the coordination of Ti^{4+} ions in titanate crystals and the Raman peak wave number corresponding to the Ti–O stretching vibration has been discussed by Sakka et al. (12). The high energy peak reflects the shortest Ti–O distance or the distortion around Ti^{4+} but it cannot be directly correlated to the coordination number of this ion. For the crystals the peaks at the highest energy are observed between 611 cm^{-1} for TiO_2 (rutile) and 905 cm^{-1} for $K_2Ti_2O_5$ (12). In contrast the Raman spectra of the titanium Nasicon-type phosphates $MTi_2(PO_4)_3$ (M = Li, Na, K) are unique and exhibit no band between 650 and 940 cm^{-1} (13, 14). In these compounds the titanium atoms are located near the center of an octahedral site sharing six common corners with six PO_4 units. The differences in the Ti–O interatomic distances are less than 0.1 Å which can explain the absence of stretching vibration at high energy.

More recently, Miyaji et al. (15) have reported an X-ray radial distribution investigation and a Raman analysis of the Na_2O-TiO_2 glasses which indicate the presence of a larger proportion of four-coordinated Ti^{4+} ions. Nevertheless the quantity of six-coordinated units is larger than in the corresponding $K_2O-2TiO_2$ and $Cs_2O-2TiO_2$ glasses. In these materials the strong peak observed at 885 cm^{-1} is attributed to the tetrahedral TiO_4 groups and the peak at 600 cm^{-1} characterizes the octahedral ones (12).

The assignment of the band at 750 cm^{-1} is less clear but its intensity increases as the fraction of TiO$_6$ octahedra increases. It could also be due to an isolated TiO$_4$ unit.

With regard to these rather complicated and conflicting conclusions a strict assignment of the emerging bands for the sodium phosphate glasses containing a larger proportion of titanium is difficult.

Nevertheless a preliminary EXAFS investigation for glasses with compositions corresponding to the AB line concludes the coexistence of two structural entities describing the titanium environment: TiO$_5$ tetragonal pyramids with a typical Ti–O short distance of 1.66 Å, TiO$_6$ octahedra with a Ti–O mean distance of 1.92 Å (19).

Ti^{4+} ions in fivefold coordination have been observed already, e.g., in Y$_2$TiO$_5$ (orthorhombic type) (20) and in K$_2$Ti$_2$O$_5$ (21). In this crystal the shortest Ti–O distance is 1.57 Å and the main peak of its Raman spectrum is observed at 905 cm^{-1} (12). TiO$_5$ pyramidal groups were also reported in the K$_2$O–TiO$_2$–SiO$_2$ glasses (22).

Therefore in the investigated glasses, the intense peaks observed in the Raman spectra at about 900 cm^{-1} are probably due to the TiO$_5$ entities, and the bands at 740 and 640 cm^{-1} may be attributed to more or less distorted TiO$_6$ octahedra.

Finally the spectra of both forms of Na$_5$Ti(PO$_4$)$_3$ (Fig. 7) can be compared. A recent structural determination of the crystalline phase (16) concluded the existence of two types of phosphates, which precludes any assignment to ν_1 and ν_3 modes in the high energy region as well as to ν_2 and ν_4 bending vibrations for the band emerging between 400 and 700 cm^{-1}.

The presence of the PO$_4$ stretching mode at a rather low energy (891 cm^{-1}) probably is due to the strongly distorted PO$_4$ tetrahedra existing in the structure. It is difficult to assign this band to the TiO$_6$ unit since the difference between the Ti–O distances is only 0.08 Å. In fact no internal mode characterizing this entity can be detected as in the case of NaTi$_2$(PO$_4$)$_3$ (13, 14).

In contrast the spectrum of the glass exhibits the typical bands previously observed and indicates the presence of TiO$_5$ and TiO$_6$ polyhedra. The strong intensity of the band peaking at 900 cm^{-1} may also indicate that the square pyramids are the prevailing entities.

In addition, the spectrum of this glass exhibits some features due to polyphosphate units such as P$_2$O$_7^{4-}$ characterized by a weak line at 1027 cm^{-1} (23).

Conclusions

Glasses existing in the Na$_2$O–TiO$_2$–P$_2$O$_5$ system can contain a significant amount of TiO$_2$. The recrystallization process investigation has allowed identification of a new crystalline phase belonging to the Nasicon-type structure Na$_5$Ti(PO$_4$)$_3$.

The spectroscopic properties of these glasses can be explained by the existence of titanium–oxygen entities such as TiO$_5$ possessing small titanium–oxygen distances and being potentially active in the nonlinear properties.

References

1. E. M. VOGEL, J. Am. Ceram. Soc. 72, 719 (1989).
2. R. ADAIR, L. L. CHASE, AND S. A. PAYNE, Phys. Rev. B 39, 3337 (1989).
3. E. M. VOGEL, S. G. KOSINSKI, D. M. KROL, J. L. JACKEL, S. R. FRIBERT, M. K. OLIVER, AND J. D. POWERS, J. Non-Cryst. Solids 107, 244 (1989).
4. A. KISHIOKA, M. HABA, AND M. AMAGASA, Bull. Chem. Soc. Jpn. 47, (10), 2493 (1974).
5. A. KISHIOKA, Bull. Chem. Soc. Jpn. 51, (9), 2259 (1978).
6. L. O. HAGMAN AND P. KIERKEGAARD, Acta Chem. Scand. 22, 1822 (1968).
7. F. CHERKAOUI, J. C. VIALA, C. DELMAS, AND P. HAGENMULLER, Solid State Ionics 21, 333 (1986).
8. R. D. SHANNON, Acta Crystallogr. Sect. A 32, 751 (1986).
9. D. E. SCAIFE, Sol. Energy 25, 41 (1980).
10. A. EL JAZOULI, thesis. University of Bordeaux I (1986).

11. V. FAWCETT, D. A. LONG, AND L. H. TAYLOR, *in* "Proceed, 5th International Conference on Raman Spectra, Freiburg, 1976" (E. Schamio, J. Branmuller, W. Kieffer, B. Schrader, and H. W. Schrotter, Eds.)

12. S. SAKKA, F. MIYAJI, AND K. FUKUMI, *J. Non-Cryst. Solids* **112,** 64 (1989).

13. Y. YONG AND P. WENQIN, *Mater. Res. Bull.* **25,** 841 (1990).

14. P. TARTE, A. RULMONT, AND C. MERCKAERT-ANSAY, *Spectrochim. Acta A* **42** (9), 1009 (1986).

15. F. MIYAJI, T. YOKO, H. KOZUKA, AND S. SAKKA, *J. Mater. Res. Sci.* **26,** 248 (1991).

16. S. KRIMI, A. EL JAZOULI, I. MANSOURI, J. P. CHAMINADE, P. GRAVEREAU, AND G. LE FLEM, submitted for publication.

17. C. DELMAS, F. CHERKAOUI, AND P. HAGEN-MULLER, *Mater. Res. Bull.* **21,** 469 (1986).

18. A. CLEARFIELD, R. GUERRA, A. OSKARSSON, M. A. SUBRAMANIAN, AND W. WANG, *Mater. Res. Bull.* **18,** 1561 (1983).

19. C. DUCHESNE AND E. FARGIN, private communication.

20. W. G. MUMME AND A. D. WADSLEY, *Acta Crystalogr. B* **24,** 132A (1968).

21. S. ANDERSON AND A. D. WADSLEY, *Acta Chem. Scand.* **15,** 663 (1961).

22. C. A. YARKER, P. A. V. JOHNSON, A. C. WRIGHT, J. WONG, R. B. GREEGOK, F. W. LYTLE, AND R. N. SINCLAIR, *J. Non-Cryst. Solids* **79,** 117 (1986).

23. R. RULMONT, R. CATHAY, M. LIEGEOIS-DUYCKAERTS, AND P. TARTE, *Eur. J. Inorg. Solid State Chem.* **28** (1), 207 (1991).